

# Comparative Analysis of Crystalline and Double-Junction Amorphous Silicon Modules Performance in Outdoor Conditions

**Cristina Cornaro**

Department of Enterprise  
Engineering and CHOSE,  
University of Rome Tor Vergata,  
Via del Politecnico,  
1, 00133 Rome, Italy  
e-mail: cornaro@uniroma2.it

**Davide Musella**

Green Utility SPA,  
Via A. Bargoni,  
78, 00153 Rome, Italy  
e-mail: davide.musella@greenutility.eu

*The paper deals with an extensive photovoltaic (PV) modules monitoring activity carried out at the outdoor station ESTER (Solar Energy TEst and Research) of the University of Rome Tor Vergata, Italy. The purpose of the work was to evaluate and compare the performance of PV silicon modules of polycrystalline (poli-Si) and amorphous (a-Si) technologies during a medium-term outdoor exposure at optimized tilt angle, facing south. Two PV modules, one polycrystalline silicon and one double-junction amorphous silicon, have been exposed since May 2009 until Oct. 2010. A complete characterization of the weather conditions at the site during the test has been performed, and the most relevant parameters for the performance comparison of the two technologies have been derived. In order to compare different technologies and power productions, the energy yield (Y) and performance ratio (PR) for the two modules have been evaluated on a monthly and yearly basis. The typical seasonal trend of PR has been observed for the polycrystalline module, essentially due to the temperature influence on the module performance. For the a-Si module, instead, a degradation trend has been observed for the first months of operation. Subsequently, a significant recovery in the PR and energy production has been registered. [DOI: 10.1115/1.4023968]*

*Keywords:* PV modules, outdoor monitoring, amorphous silicon, polycrystalline silicon

## 1 Introduction

Many PV modules manufacturers are present on the market, claiming high performance and high reliability of their products. The module specifications are restricted to the standard test conditions (STC), which are not very representative of the real conditions in which the PV devices have to operate. It has been proven by various work in the literature that the PV modules' performance depends on their technology, the location, the weather conditions, and the mounting configuration [1–4]. The behavior of thin-film devices, such as amorphous silicon (a-Si), cadmium telluride, and copper indium selenide are still not very well understood [5,6] and require more research. Moreover, new emerging technologies, like polymeric and organic solar cells, are requesting a wide research activity to better understand their behavior in the outdoor conditions. Therefore, it is important to produce and disseminate results about the real behavior of photovoltaic devices in outdoor conditions at various locations through reliable and accurate measurements. Results can be useful for designers and customers to choose the right device for their specific application.

In Europe, there are well-established laboratories that are doing research on the performance of PV modules of well-consolidated technologies as well as new emerging ones. Some of the representative results are presented in Refs. [7–9]. More recently, an outdoor monitoring facility, called ESTER [10], for testing PV modules of various technologies has been built at the University of Rome, Tor Vergata, Italy, and it is part of the laboratories of the Centre for Hybrid and Organic Solar Energy (CHOSE), a center born in 2006 and funded by the Lazio Region with the objective of giving impulse to the photovoltaic research and

industry in Italy and especially to develop and industrialize the dye-sensitized solar cells as a new generation of photovoltaic technology. The present paper illustrates the results of a monitoring activity started in May 2009 with the objective to evaluate and compare the performance of a polycrystalline (poli-Si) PV module of well-established technology and a double-junction amorphous silicon (a-Si) PV module of the second generation of photovoltaic devices. The test covered a time period between May 2009 and Oct. 2010.

## 2 Materials and Methods

**2.1 Experimental Setup.** The ESTER outdoor station is shown in Fig. 1. It consists of three separate units, as showed in the figure: a solar-weather unit; a spectral unit; and a PV monitoring unit.

The solar-weather unit provides values of the three separate components of solar irradiance (direct, diffuse, and reflected) and the global solar irradiance on a horizontal plane together with the standard weather parameters of air temperature, relative humidity, pressure, wind velocity and direction, and rain gauge.

The spectral unit, recently added, consists of two EKO spectroradiometers, which measure the spectral irradiance on a horizontal plane in the spectral range between 350 nm and 1700 nm.

The PV monitoring unit is provided with two stands that allow one to expose approximately eight modules of medium size, in total. The stand No. 1 is a south-oriented frame with variable tilt, while the stand No. 2 is a sun tracker. Both stands are equipped with irradiance sensors (pyranometers and reference cells of various technologies) and have local weather stations, installed nearby, as evidenced in the figure.

The architecture of the data acquisition system is shown in Fig. 2 for the three separate units. At the PV monitoring unit, each PV module under test is kept at the maximum power point of

Contributed by the Solar Energy Division of ASME for publication in the JOURNAL OF SOLAR ENERGY ENGINEERING. Manuscript received September 5, 2012; final manuscript received February 28, 2013; published online June 11, 2013. Assoc. Editor: Santiago Silvestre.

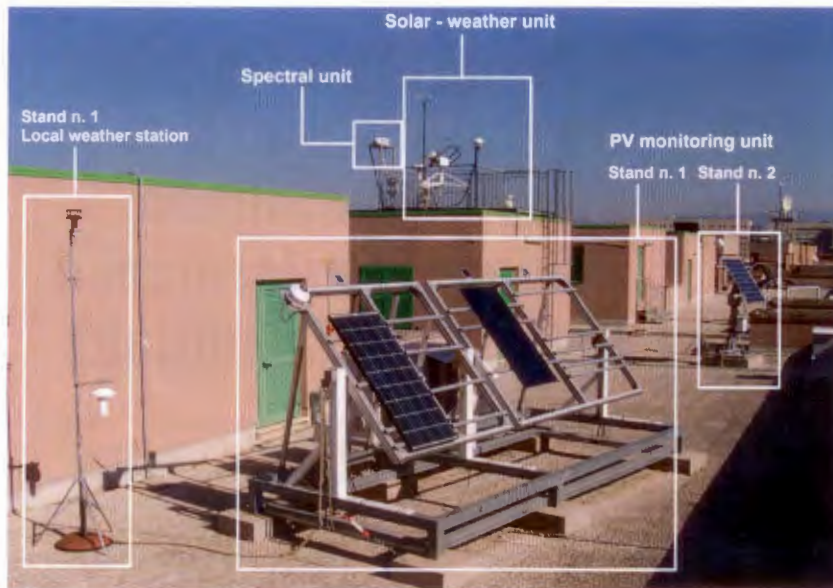


Fig. 1 Overview of the ESTER station

operation by a dedicated maximum power point tracker (MPPT) electronic device, which provides measurements of  $P_{max}$  at a time rate of 1 min, while every 10 min, it traces the IV curve of the device. Dedicated analog-to-digital (A/D) converters extract the data coming from the environmental sensors of irradiance (EKO pyranometers and IKS reference cells calibrated by the Institute for Solar Energy Supply Technology (ISET)), air and module temperature, and wind velocity and direction at the same time rate of 1 min. Data acquisition of the PV monitoring unit is managed by a CR1000 data logger from Campbell Scientific that downloads the data in three dedicated tables of a server database built using MySQL platform.

The solar-weather unit data acquisition is managed by a CR10 data logger from Campbell as well, synchronized with the CR1000. The acquisition system downloads the solar-weather data in another two specific tables of the same database.

At the time of the test, the spectral unit, consisting of the two EKO spectroradiometers, was managed separately by a dedicated computer using software provided by the manufacturer. A subsequent upgrading of the system consisted of the substitution of the dedicated computer with another CR1000 synchronized with the other units that downloads spectral data in the same database of the other two units. A detailed analysis of the uncertainty sources

of all the instrumentation of the PV monitoring unit was performed together with the validation of the system [11].

The monitoring activity presented in this work was started in Apr. 2009, and data analysis is presented from May 2009 until Oct. 2010. A double-junction amorphous silicon device from EPV Solar (EPV-50) was mounted on Stand 1, where a polycrystalline silicon module by Kyocera (KC125-GHT) was already exposed since Jan. 2008, as shown in Fig. 1. Tilt angle was varied each month in order to optimize energy collection and simultaneously provide normal incidence at noon. The back of the module temperature was measured, attaching a Pt100 sensor on the back of each module using a metallic tape. In-plane irradiance was collected by the EKO pyranometer. Electrical parameters measured every minute by the MPPT at the maximum power point were considered for the analysis.

**2.2 Data Analysis.** Data coming from the PV modules monitoring unit are extracted from the database using a made-on-purpose software, called Noria [12]. Noria was conceived in order to simplify data recognition and interpretation. Virtually reproducing the station hardware and each configuration of the tests performed during time, the software can correctly recognize the data in the database and extract them through logical queries. Data extracted for the present work were sorted only by date and PV module type, archiving them on a monthly basis.

Data sorted by the Noria software were then filtered by a filtering procedure implemented using a Matlab code. In Fig. 3, the raw and filtered data of the electrical power versus irradiance for the month of July 2009, are showed, as an example, for the KC125 and EPV-50 modules, respectively. The typical linear trend is recognized; however, a high data aggregation is visible at low irradiance for the raw data (light gray). Shadowing and/or reflection from the surroundings are responsible for this deviation from the linear trend, causing data disturbance. Moreover, certain dispersion in the data can be observed, especially at medium irradiance values, probably due to fluctuation of the environmental parameters and to the oscillation of the power point tracking system (MPPT). The filtering procedure eliminates data out of the physical range limits, data coming from system fault, and also outliers and shadowing effects through statistical analysis. The resulting filtered data are the black dots shown in the graphs of Fig. 3 for the two modules. Besides that, solar irradiance lower than  $20 \text{ W/m}^2$  was discarded. The filtering procedure was applied to the data of the KC125 and EPV-50 modules archived on a monthly basis for a period of 18 months.

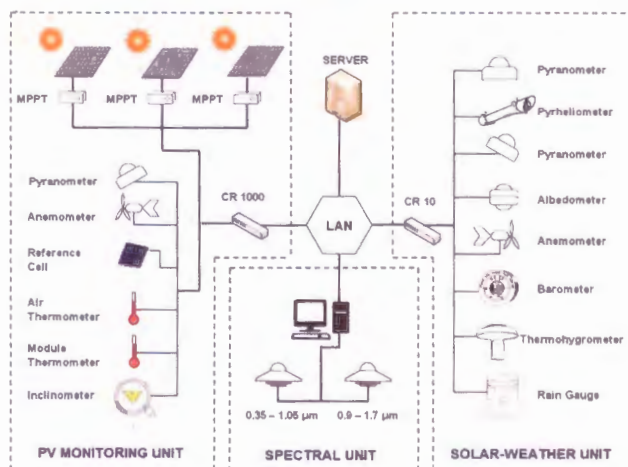


Fig. 2 Layout of the data acquisition system

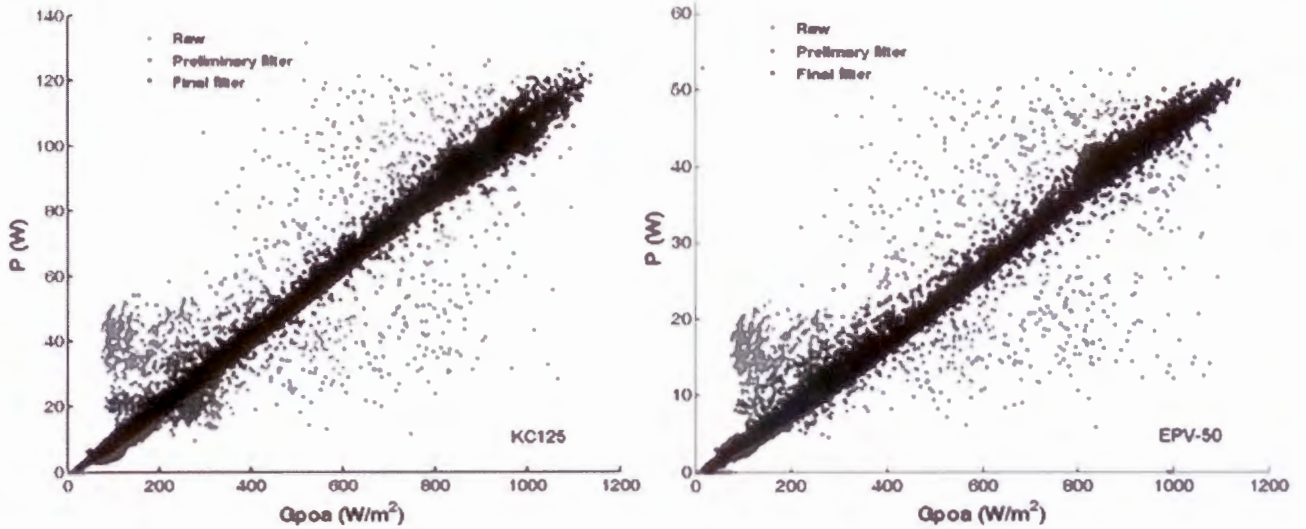


Fig. 3 Raw and filtered power data versus in-plane irradiance for KC125 and EPV-50. Filtering data procedure applied to the month of July 2009.

### 3 Results and Discussion

**3.1 Climatic Characterization.** A detailed climatic characterization was carried out for the 18 months of monitoring. Ambient temperature and irradiance were treated to get the average ambient temperature and irradiation evaluated at various in-plane irradiance classes ( $G_{poa}$ ), as shown in Fig. 4. On the whole, during the test, the incident irradiation ( $I$ ) was of the order of  $2.2 \text{ MWh/m}^2$ , with consistent high energy collected at high irradiance values. This is due to the fact that, in the 18 months of test, we have two summer periods that increase the high irradiance contribution.

To characterize the weather conditions during the test period, the ratio of diffuse irradiance on a horizontal plane over the global irradiance on the same plane was evaluated for each minute of acquisition. This ratio, called cloud ratio ( $CR$ ), gives an indication of the amount of diffuse irradiance during time [13].  $CR$  varies from 0 to 1, and this range has been divided into five classes, each of them representing a particular weather condition that can be attributed to the time in which the data have been collected.  $CR$  values near 1 are indicatively representative of bad weather conditions, while  $CR$  values near 0 indicatively represent clear sky conditions. Figure 5 shows the five  $CR$  classes observed for

each month of the test. A higher percentage of clear sky instants is mainly found during summer.

It can be observed that the spring months of the year 2010 present less favorable weather with a high percentage of cloudy days.

**3.2 PV Performance Indices.** To evaluate the performance of PV modules of various technologies, a series of indices can be considered. The main index used in the absence of direct measurements on the module is the efficiency at standard test conditions (STC). These conditions are values of irradiance ( $1000 \text{ W/m}^2$ ), module temperature ( $25^\circ\text{C}$ ), and air mass (AM 1.5), considered as reference for modules' properties evaluation.

The efficiency at STC is defined as

$$\eta_{\text{STC}} = \frac{P_{\text{nom}}}{A \cdot G_{\text{STC}}} \quad (1)$$

where  $P_{\text{nom}}$  is the nominal power (or peak power) at STC,  $A$  is the surface area of the module, and  $G_{\text{STC}}$  is the irradiance of  $1000 \text{ W/m}^2$ . This efficiency can be derived from the specification given by the manufacturer or can be evaluated through indoor measurements using a sun simulator [14].

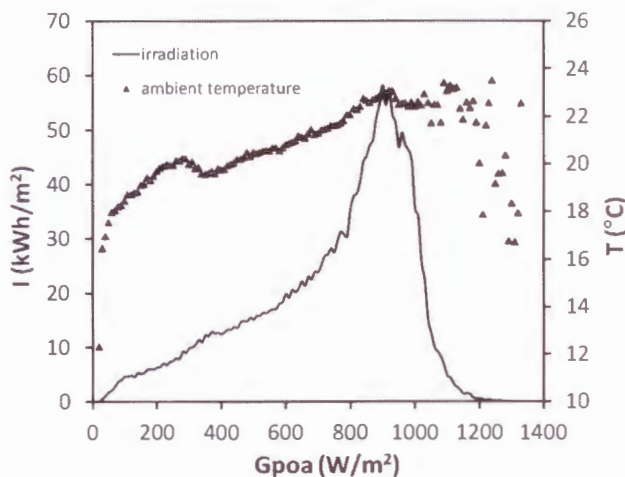


Fig. 4 Irradiation and average ambient temperature evaluated at different irradiance classes for the period of test

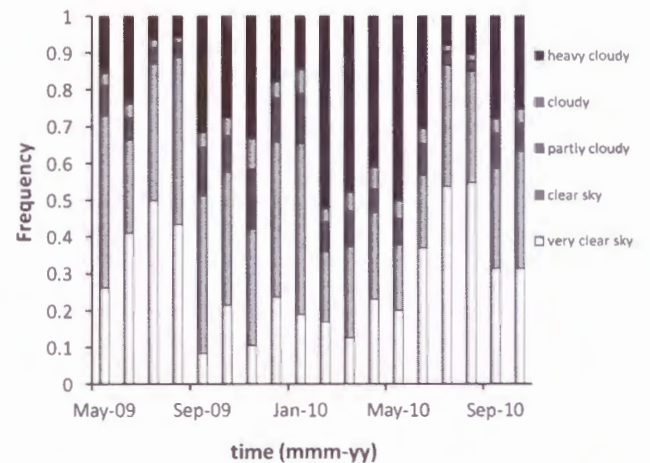


Fig. 5 Cloud ratio frequency evaluated for each month of the test

When the PV module is working in the real environment at its maximum power point, its real efficiency can be defined as follows:

$$\eta = \frac{P_{\max}}{A \cdot G_{\text{poa}}} \quad (2)$$

where  $P_{\max}$  is the PV module electrical power produced at the maximum power point of operation and  $G_{\text{poa}}$  is the correspondent in-plane irradiance. The above-mentioned indices evaluate the module performance instantaneously, but they can also give information about the performance in a defined period of time. In this case, instead of electrical power and irradiance, the correspondent energy values in the defined period of time (day, month, or year) have to be evaluated. The efficiency indicates the performance of a device, but it does not give indications about its energy production. If one wants to evaluate and to compare the energy production of different modules of different power size, the energy yield is the suitable parameter to use. The energy yield ( $Y$ ) is written as

$$Y = \frac{E}{P_{\text{nom}}} [\text{kWh/kW}] \quad (3)$$

where  $E$  is the electrical energy produced by the module in a defined time interval and  $P_{\text{nom}}$  is the nominal power. This index can also be interpreted as the number of hours in which the PV modules work at their peak power value. Since the energy production is normalized to the module size, this index allows comparing PV devices of different peak powers, as already said.

It is well known that the energy production of a PV module does not depend only on radiation intensity but also, to some extent, on the temperature of the module, the variation of solar spectrum, and also other factors that do not strictly depend on the module itself. To take into account all these influences, another index, called performance ratio ( $PR$ ), is defined [15],

$$PR = \frac{Y}{Y_r} \quad \text{with} \quad Y_r = \frac{I}{G_{\text{STC}}} \quad (4)$$

$Y_r$  is called the reference yield and is the ratio between the irradiation evaluated in the considered time interval and the irradiance at STC; it also represents the sun peak hours defined as the hours in which the in-plane irradiance has reached  $1000 \text{ W/m}^2$ . The  $PR$  index can also be seen as the ratio of the real efficiency over the efficiency at STC, and for this reason, it measures how far is the behavior of the module with respect to its performance at STC. As already mentioned, this index is not sensitive to irradiance variation but to secondary effects on the module performance.

**3.3 Discussion of the Results.** For the KC125 and the EPV-50 modules, the monthly yield and performance ratio have been calculated and are shown in Figs. 6 and 7. From the graph of Fig. 6, it can be noted the low energy production of the two modules during the winter period, which corresponds to lower peak sun hours (reference yield ( $Y_r$ )), also showed in the graph. The high yield observed in Aug. 2009 for KC125 is mainly due to the higher time of operation evaluated for this module, with respect to EPV-50. Indeed, a failure of the MPPT that managed the EPV-50 was observed and many data were discarded by the filtration procedure. Since each module is subjected to filtration separately, different amounts of data were cut for the two modules. Also, for May and June 2010, a lower energy production can be observed with respect to the same months of 2009, and this is mainly due to the worst weather conditions experienced for these months in 2010.

The effect of degradation of amorphous silicon can be better seen from the monthly  $PR$  trend. Since the first exposure in Apr. 2009, the EPV-50 has lost approximately 13% of  $PR$  in one year. It appears quite clear that, for the first 4 months, a degradation

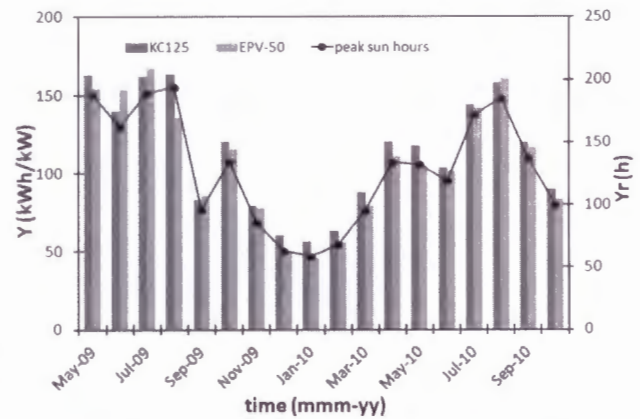


Fig. 6 Monthly yield calculated for the KC125 and the EPV-50 modules

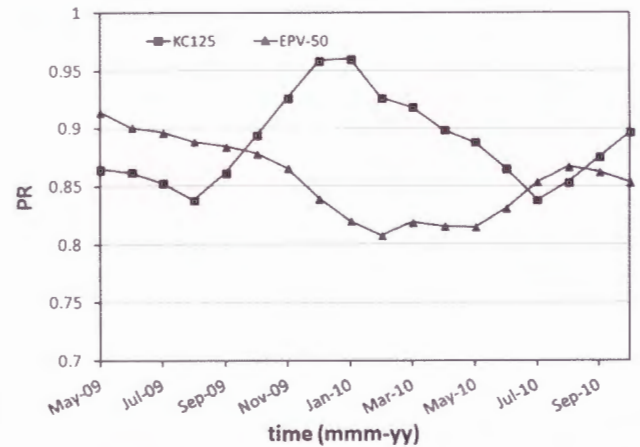


Fig. 7 Monthly performance ratio ( $PR$ ) calculated for the KC125 and the EPV-50 modules

effect can be observed, while for the other months, until Apr. 2010, a combined effect of seasonal variation and degradation can be considered. Both modules exhibit a typical seasonal effect due to their performance dependence on temperature and/or solar spectrum. It is well known that, for poli-Si, high temperature reduces module production, and this is the reason why the  $PR$  for KC125 is higher during the cold season than during the hot season (see Fig. 8). Moreover, not significant degradation has been observed for this module, which has been already tested in

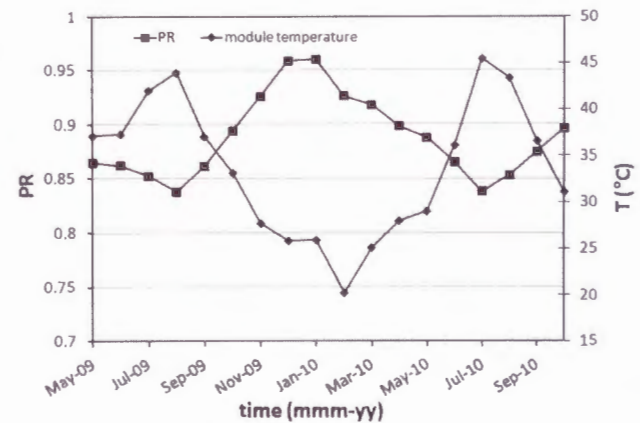


Fig. 8 Monthly performance ratio ( $PR$ ) calculated for the KC125 and monthly average module temperature

Lugano since the year 2006–2007 [16]. On the contrary, the amorphous silicon seems to respond better to higher temperatures with respect to poli-Si, even if for the first four hot months of operation, the initial degradation trend due to light exposure (Staebler–Wronski effect) [17] can be observed. To quantify this effect, the IV curves constantly measured during the exposure period were used. Every 15 days, during the test period, IV curves collected at normal incidence (between 11.30 and 13.30) and during clear days and stable irradiance (only 1% variation in two consecutive minutes) were selected. The curves were then translated to STC using the Blaesser method [18]. Figure 9 shows the trend of the STC power obtained by the translation procedure, normalized to its initial value (initial power fraction) versus time. A decreasing trend can be observed that is quantified in approximately 4% of degradation. In this period, degradation due to the Staebler–Wronski effect is predominant. Later on, a principal of seasonal oscillation can be recognized. This trend could be partly explained by the seasonal temperature effect of annealing that partially recovers power degradation during summer (due to high temperatures) and partly by the seasonal variation of the solar spectrum, which is bluer in summer (better match with the spectral response of amorphous silicon), as already discussed by other authors, as, for example, in Refs. [19] and [20]. For these reasons, the summer period of 2010 contributed to partially recover the initial degradation induced by light soaking.

Table 1 summarizes the annual performance of the two modules tested together with their performance after 12 months and 18 months of operation. The PR uncertainty was evaluated applying the error propagation theory and is in the order of  $\pm 5\%$ . The measurement uncertainty of the STC power has not been considered here. The main contribution to overall uncertainty is coming from the pyranometer irradiance measurements (dependent on the irradiance range: approximately  $\pm 5\%$  in the average) and in a smaller amount from the current and voltage measurements ( $\pm 0.2\%$  for both measurements) [21]. The uncertainty on the yield is the one referred to the measurements of the module power that, from the MPPT specification, is fixed to  $\pm 0.5\%$ . From these considerations, it can be concluded that the two PV modules present the

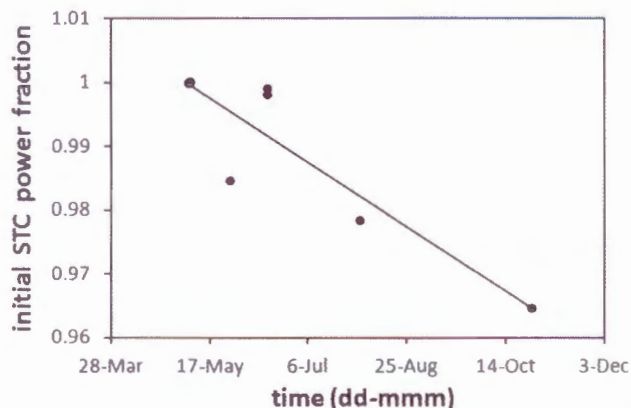


Fig. 9 Initial STC power fraction of the EPV-50 amorphous silicon module for the first four months of operation in real operating conditions

Table 1 Summary of the modules performance

PV module	12 months			18 months		
	$Y$ (kWh/kW)	$\eta$ (%)	$PR$	$Y$ (kWh/kW)	$\eta$ (%)	$PR$
KC125GHT	1297	11.9	0.88	2030	11.8	0.88
EPV-50	1231	4.6	0.87	1939	4.6	0.86

same annual PR and that the double junction amorphous silicon module produced approximately 5% less energy than the poli-Si.

This is partly due to a failure of the MPPT that managed the EPV module during Aug. 2009 and partly to the initial degradation of the module.

## 4 Conclusions

An extensive monitoring campaign was carried out on two photovoltaic modules of different technologies with the aim to better understand their behavior in real operating conditions and to contribute to the dissemination of this information to a wider audience. It has to be pointed out that the results obtained cannot be extended to every module of the considered technology, since many differences can be encountered in terms of performance and energy production also among modules of the same technology but of different manufacturers. However, some basic trends can be recognized in the tested devices. The polycrystalline module was proven to be highly stable and with an average annual PR of 0.88. A seasonal trend in the monthly PR was observed due to the temperature effect on the module performance; these seasonal effects, however, compensate each other when the annual behavior of the module is considered. The double junction amorphous silicon module shows an effect of degradation in the first months of operation, and this effect is partially recovered during the hot months of 2010. Even if the monthly PR trend can be used to recognize the degradation, the PR on an annual basis is the same of the annual PR of poli-Si. On an annual basis, the a-Si module produced approximately 5% less energy than the poli-Si, and for the summer months of 2010 (June–September), the a-Si produced the same amount of energy per unit of nominal power as the poli-Si (within 3%).

## Acknowledgment

This work was supported by the Lazio Region within the frame of the Centre for Hybrid and Organic Solar Energy (CHOSE).

## Nomenclature

- $A$  = module surface area (m)
- $CR$  = cloud ratio
- $E$  = energy produced by the module (Wh)
- $G_{\text{poa}}$  = in-plane irradiance ( $\text{W}/\text{m}^2$ )
- $G_{\text{STC}}$  = irradiance at standard test conditions ( $\text{W}/\text{m}^2$ )
- $I$  = irradiation ( $\text{Wh}/\text{m}^2$ )
- $P_{\text{max}}$  = electrical power at the maximum power point (W)
- $P_{\text{nom}}$  = nominal electrical power (W)
- $PR$  = performance ratio
- $T$  = temperature ( $^{\circ}\text{C}$ )
- $Y$  = yield (kWh/kW)
- $Y_r$  = reference yield (h)
- $\eta$  = module efficiency (%)
- $\eta_{\text{STC}}$  = module efficiency at standard test conditions (%)

## References

- [1] Jardine, C. N., Conibeer G. J., and Lane, K., 2001, "PV-COMPARE: Direct Comparison of Eleven PV Technologies at Two Locations in Northern and Southern Europe," Proceedings of the 17th European Conference on Photovoltaic Solar Energy Conversion, Munich.
- [2] Gottschalg, R., del Cueto, J. A., Betts, T. R., and Infield, D. G., 2005, "Seasonal Performance of A-Si Single and Multijunction Modules in Two Locations," Proceedings of the 31st IEEE PV Specialists Conference, Buena Vista, FL, January 3–7.
- [3] Carr A. J., and Pryor, T. L., 2004, "A Comparison of the Performance of Different PV Module Types in Temperate Climates," Sol. Energy, **76**, pp. 285–294.
- [4] Zdanowicz, T., Rodziewicz, T., and Zabkowska-Waclawek, M., 2004, "Effectiveness of the Sun Tracking Option During Different Insolation Periods," Proceedings of the 19th European Photovoltaic Solar Energy Conference, Paris, June 7–11.
- [5] Longden, D., Aitchison, L., Gottschalg, R., and Infield, D. G., 2004, "Long-Term Performance of a CdTe Array," Proceedings of the 19th European Photovoltaic Solar Energy Conference, Paris, June 7–11.

- [6] Zdanowicz, T., Prorok, M., Kolodenny, W., Stellbogen, D., and Schaeffler R. R., 2005, "Evaluation of Performance Parameters of CIS Modules Using Long-Term Outdoor Monitoring Data," Proceedings of the 20th European Photovoltaic Solar Energy Conference, Barcelona, June 6–10.
- [7] Chianese, D., Friesen, G., Pasmelli, P., Pola, L., Realini, A., Cereghetti, N., and Bernasconi, A., 2007, "Direct Performance Comparison of PV Modules," Proceedings of 22nd EPVSEC, Milano, September 3–7.
- [8] Betts, T. R., Zdanowicz, T., Prorok, M., Kolodenny, W., de Moor, H., v.d. Borg, N., Stellbogen, D., Hohl Fbinger, J., Warta, W., Friesen, G., Chianese, D., Guerin de Montgareuil, A., Herrmann, W., Diaz Berrade, J., Moracho, J., Cuchi, A. B., Lagunas, A. R., and Gottschalg, R., 2006, "Photovoltaic Performance Measurements in Europe: PV Catapult Round Robin Tests," IEEE 4th World Conference on Photovoltaic Energy Conversion, Waikoloa, HI, May 7–12.
- [9] Dunlop, F. D., and Halton, D., 2006, "The Performance of Crystalline Silicon Photovoltaic Solar Modules After 22 Years of Continuous Outdoor Exposure," *Prog. Photovoltaics*, **14**, pp. 53–64.
- [10] Spina, A., Corwar, C., and Serafini, S., 2008, "Outdoor ESTER Test Facility for Advanced Technologies PV Modules," Proceedings of the 33rd IEEE PV Specialists Conference, San Diego, CA, May 11–16.
- [11] Spina, A., Comaro, C., Intreccialaghi, G., and Chianese, D., 2009, "Data Validation and Uncertainty Evaluation of the ESTER Outdoor Facility for Testing of PV Modules," Proceedings of the 24th European Photovoltaic Solar Energy Conference and Exhibition, Hamburg, Germany, September 21–24.
- [12] Spina, A., Comaro, C., and Trani, P. G., 2008, "Noria Data Management Software for PV Modules Characterization in the Outdoor ESTER Test Facility," Proceedings of the 23rd European Photovoltaic Solar Energy Conference and Exhibition, Valencia, Spain, September 1–5.
- [13] Rahim, R., Baharuddin, and Mulyadi, R., 2004, "Classification of Daylight and Radiation Data into Three Sky Conditions by Cloud Ratio and Sunshine Duration," *Energy Build.*, **36**, pp. 660–666.
- [14] IEC, 2007, "Photovoltaic Devices—Part 2: Requirements for Reference Solar Devices," IEC Paper No. 60904-2.
- [15] Marion, B., Adelstein, J., Boyle, K., Hayden, H., Hammond, B., Fletcher, T., Canada, B., Narang, D., Shugar, D., Wenger, H., Kimber, A., Mitchell, L., Rich, G., and Townsend, T., 2005, "Performance Parameters for Grid-Connected PV Systems," Proceedings of the 31st IEEE Photovoltaics Specialists Conference, Lake Buena Vista, FL, January 3–7.
- [16] Comaro, C., Musella, D., Chianese, D., Friesen, G., and Dittmann, S., 2010, "Outdoor PV Module Performance Comparison at Two Different Locations," Proceedings of the AMSE ATI-UIT2010 Conference on Thermal and Environmental Issues in Energy Systems, Sorrento, Italy, May 16–19.
- [17] Staebler, D. L., and Wronski, C. R., 1977, "Reversible Conductivity Changes in Discharge Produced Amorphous Si," *Appl. Phys. Lett.*, **31**(4), pp. 292–294.
- [18] Blaesser, G., and Zaiman, W., 1991, "On Site Power Measurement on Large PV Arrays," 10th European Solar Energy Conference, Lisbon, Portugal, April 8–12.
- [19] Minemoto, T., Nagae, S., and Takakura, H., 2007, "Impact of Spectral Irradiance Distribution and Temperature on the Outdoor Performance of Amorphous Si Photovoltaic Modules," *Sol. Energy Mater. Sol. Cells*, **91**, pp. 919–923.
- [20] Gottschalg, R., Betts, T. R., Toftsd, D. G., and Keece, M. J., 2005, "The Effect of Spectral Variations on the Performance Parameters of Single and Double Junction Amorphous Silicon Solar Cells," *Sol. Energy Mater. Sol. Cells*, **85**, pp. 415–428.
- [21] Intreccialaghi, G., 2007, "Prime Misura Outdoor su un Modulo Fotovoltaico di Corrente Produzione Industriale," Laurea thesis, University of Rome Tor Vergata, Rome.